Behaviour of pumice sand during hydrostatic and K_o compression

Comportement du sable de pierre ponce lors de la compression K_o

N. Kikkawa, M.J. Pender & R.P. Orense
University of Auckland, New Zealand

E. Matsushita
Nagano National College of Technology, Nagano, Japan

ABSTRACT

In order to understand the characteristics of pumice sand, we scanned pumice particles using micro X-ray computed tomography (X-ray CT), which showed that pumice particles have not only surface voids but also internal voids. Therefore, pumice sand is lighter than quartz sands and also is crushable. In addition, from our previous research, the relative density of pumice sand can not be estimated from conventional CPT testing. Because of this unique behaviour, there is a need for more experimental study of this material to fully understand its geotechnical properties. First, we performed hydrostatic compression tests on loose pumice sand and monitored the volume change with elapsed time during loading and unloading. After these tests, the particle-size distribution (PSD) was measured. Second, in order to distinguish the differences in stress relaxation between loose and dense sand which might occur during CPT testing, K_o compression tests were performed at various displacement rates, from 0.5mm/min to 25mm/sec. The final compression was about 33% of the original length of the specimens. After compression, the maximum displacement was held constant for a specified period of time and the relaxation of the axial stress was monitored during this time. From these results, the stress relaxation of loose sand was slightly larger than that of dense sand, presumably because loose sand has more spaces for rearrangement of particles during the stress relaxation process.

RÉSUMÉ

Afin de présenter les propriétés du sable de pierre ponce, nous avons observé une particule de pierre ponce par micro tomographie a rayon X. Nous avons ainsi pu montrer que les particules de pierre ponce ne présentent pas uniquement des pores internes mais également des pores surfaciques. Ainsi, le sable de pierre ponce est plus léger que les autres sables siliceux mais il est aussi broyable. Nous avons montre au cours de travaux précédents que la densité relative des sables de pierre ponce ne peut être estimée par des moyens CPT conventionnels. De ce fait, d'autres expérimentations sont nécessaires pour comprendre pleinement ses propriétés géotechniques. Dans un premier temps, nous avons réalisé un test de compression isotrope sur des particules de sable de pierre ponce lâche et étudié les variations de volume en fonction du temps lors des chargements et déchargements. La granulométrie (PSD) a été mesurée. Lors du compactage se produisent non seulement un réarrangement des particules mais aussi une déformation élastique des particules elles-mêmes. Dans un second temps, afin d'identifier les différences lors du relâchement des contraintes pour des sables denses et lâches, des test de compression K_o ont été exécutés avec des vitesses de déplacements allant de 0.5 mm/min a 25 mm/sec. La compression finale avoisinait 33% de la longueur initiale des échantillons. Apres compactage, le déplacement maximal a été maintenu constant pendant une durée spécifiée et le relâchement des contraintes axiales en fonction du temps a été mesuré. Celui-ci est plus important pour le sable lâche que pour le sable dense. Ainsi, le sable lâche possède plus d'espace pour réarranger les particules lors du relâchement des contraintes.

Keywords : pumice sand, stress relaxation, displacement rate, relative density, particle crushing

1 INTRODUCTION

Pumice deposits are found in several areas of the North Island of New Zealand. They originated from a series of volcanic eruptions centred in the Taupo and Rotorua regions of the central North Island. The pumice material has been distributed initially by the explosive power of the eruptions and associated airborne transport; this has been followed by erosion and river transport. Presently, pumice deposits exist mainly as deep sand layers in river valleys and flood plains, but are also found as coarse gravel deposits in hilly areas. Although they do not cover wide areas, their concentration in river valleys and flood plains means they tend to coincide with areas of considerable human activity and development. Thus, they are frequently encountered in engineering projects and their evaluation is a matter of considerable geotechnical interest.

Pumice sand is a crushable material as the individual grains of pumice may be readily crushed against a hard surface by fingernail pressure presumably because the particles have internal voids. Wesley (2001) investigated the specific gravity of pumice sand of various particle sizes using the NZ standard method with and without vacuum air extraction. He observed that the specific gravity of pumice sand decreased with increasing particle size, indicating that the proportion of internal voids increased with increasing particle size. In addition, he noted that because the specific gravity of the soil particles measured by both methods was not the same as that of quartz (which is about 2.65), even when the particle size was 0.04mm, some internal voids must be present even in very small particles. Thus, it is necessary to distinguish between internal voids and voids consisting of spaces between particles. Then, when a particle is crushed, the voids would increase because the internal voids would be exposed and manifest themselves as voids between particles.

Moreover, it is known that pumice sand is characterised by soft vesicular grains of low crushing strength, giving the material high void ratios and high compressibility. Previous research showed that the q_c values obtained from cone penetration tests (CPT) on pumice sand were only marginally influenced by the density of the material, as shown in Figure 1. We think the reason for this behaviour is that the stresses imposed by the penetrometer are so severe that particle

Proceedings of the 17th International Conference on Soil Mechanics and Geotechnical Engineering
M. Hamza et al. (Eds.)

doi:10.3233/978-1-60750-031-5-812

breakage forms a new material and that the properties of this are nearly independent of the initial state of the sand. It is also noted that pumice sand CPT resistance shows very gentle increase with confining stress as compared to normal (i.e. hard grained) sands (Wesley et al. 1999). Thus, conventional relationships between the q_c value, relative density, and confining stress are not valid for these soils. Therefore, alternative relationships specifically for pumice sands need to be developed.

In this study, compression and stress relaxation testing were performed on loose and dense pumice sand using a simple K_o triaxial cell. The effect of various constant displacement rates (0.5mm/min ~ 25mm/sec) on the response was also examined. This study was undertaken to supplement the test results obtained by Pender (2006).

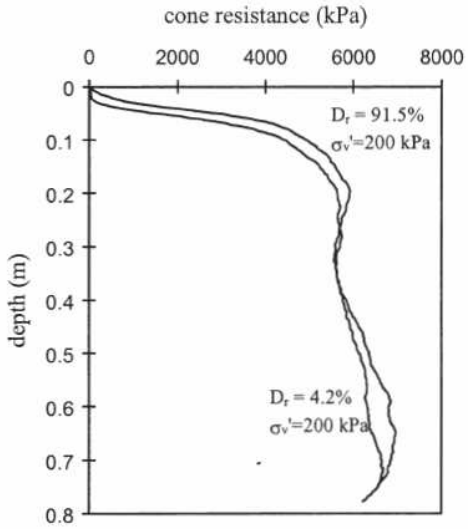

Figure 1. CPT resistance obtained from calibration chamber testing of loose and dense pumice sand (Wesley et al., 1999).

2 SAND USED AND TEST PROGRAM

2.1 *Characteristics of pumice particle from X-Ray CT scan*

In order to investigate the characteristics of pumice, we scanned pumice particles using an X-ray CT scanning machine. The result for one particle of length about 4.3mm is given here.

Figure 2 shows a horizontal cross-sectional binary image of the pumice particle. It can be observed that there are not only surface voids but also internal voids. The surface voids are interconnected with the outside surface but the internal voids are not connected with the outside surface. Figure 3 shows the three-dimensional image of the particle and the internal voids. This 3-D image was reconstructed by stacking cross-sectional images one on top of another. The internal voids were extracted by image analysis (Kikkawa et al. 2008) and are shown by the brown colour in Figure 3. The internal void ratio, i.e. the ratio of the volume of internal voids to solid particle, was calculated from the number of voxels which were considered to represent internal voids and solid particle respectively. The internal void ratio obtained was 0.02. The presence of these surface and internal voids makes the pumice particles easily deformable.

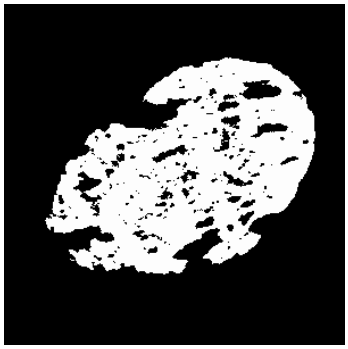

Figure 2. Cross-sectional binary image of one pumice particle.

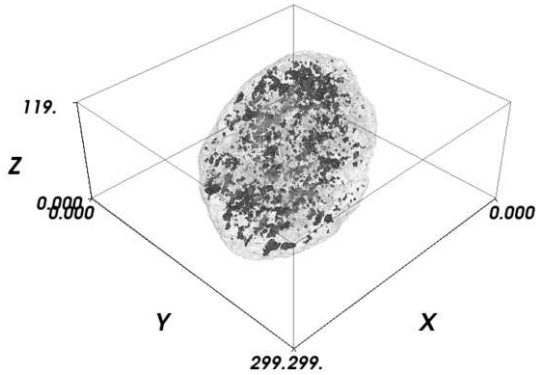

Figure 3. 3-D image of a single pumice particle with the internal voids, which are shown by brown colour.

2.2 *Engineering properties of pumice*

Figure 4 shows the particle size distributions (PSD) of pumice sands used in this study, representing those before and after testing. Only sands passing through the 1.18 mm sieve were used, with only 5.8% of the sand finer (by weight) than 63μm. Table 1 shows the physical properties of pumice sand obtained using the NZ standard method (NZS, 1988), but without a surcharge when determining the maximum dry density.

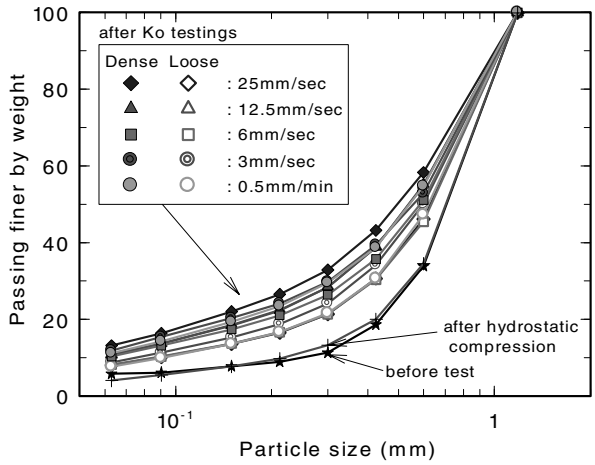

Figure 4. Particle-size distribution (PSD) of pumice sand before and after testing

Table 1. Physical properties of pumice sand.

Material	Estimated Specific Gravity	Maximum unit weight, kN/m^3	Minimum unit weight, kN/m^3
Pumice sand	1.77	6.95	5.65

2.3 *Test program*

2.3.1 *Hydrostatic compression test*

For hydrostatic compression testing, we used a conventional triaxial cell. The specimen, 75mm in diameter and 150 mm high, was prepared by the water pluviation method. Before pluviation, an appropriate mass of the dry sand was split into 8 portions and each was poured into a flask with water and then it boiled and

saturated by vacuum. After that, each layer was poured into the mould from the top end of the mould whose height was around 150mm. The mould was lined with a rubber membrane, held against the internal surface of the mould by vacuum, and the inside was filled with de-aired water to the top end of mould. The specimens were found to be fully saturated since all of the specimens had Skempton's *B*-value higher than 0.96. However the internal voids within the pumice particle could not be saturated because the internal voids are not interconnected with outside surface (Wesley 2001).

The density of specimens was in the range ρ_d= 552 ~ 598 kg/m^3. After the specimens were prepared, hydrostatic compression was performed to 10, 20, 50, 100, 200, 400, 800 and 1600 kPa effective consolidation pressures and then the pressure was unloaded until 10kPa effective consolidation pressure. At each pressure, the volume change with elapsed time was monitored.

2.3.2 *K_o compression and stress relaxation testing*

Figure 5 shows a schematic diagram of the K_o triaxial cell used in this study. The concept of this test apparatus is based on that developed by Davis & Poulos (1964). The inside of the triaxial cell was filled with water and the diameter of the loading ram and specimen were the same; therefore, radial deformation was restricted because the cell water is incompressible.

The specimens, 75 mm in diameter and 150 mm tall, were tested dry. The density of the specimen was varied by employing two specimen preparation methods. For both methods, the sand sample was split into 8 sub-specimens and each sub-specimen was pluviated into the mould lined with a rubber membrane. For loose specimens, air pluviation was used and each sub-specimen was pluviated from a height of 0 mm above the top end of the specimen using a funnel. For dense specimens, each sub-specimen was pluviated in air from a height of 100 mm, and then densified by tapping the base of the triaxial cell with a rubber hummer. This process resulted in two sets of pumice samples: loose (ρ_d= 605~641 kg/m^3) and dense (ρ_d= 663~704 kg/m^3) samples.

Next, the interior of the triaxial cell was filled with water and an initial cell pressure of 50 kPa was applied and the cell pressure valve closed. The specimens were compressed at various displacement rates (0.5 mm/min, 3 mm/sec, 6 mm/sec, 12.5 mm/sec and 25 mm/sec) until an axial deformation of 50 mm was reached, which is equivalent to 33% axial strain. Immediately after, the 50 mm axial deformation was held constant and the decrease in axial stress and confining pressure was monitored with time. After the specified time, the specimen was unloaded and, at the end of the test, the PSD of specimen was measured.

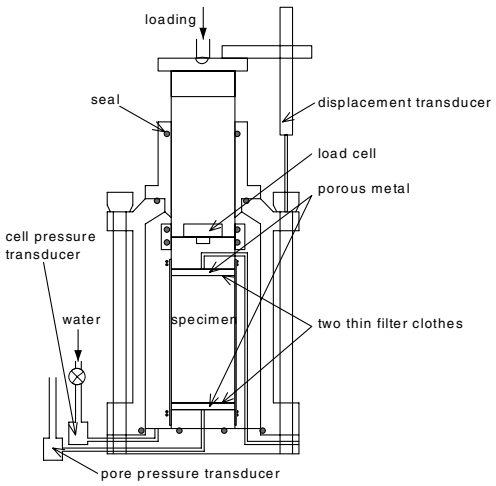

Figure 5: Schematic diagram of K_o triaxial cell equipment.

3 TEST RESULTS AND DISCUSSION

3.1 *Hydrostatic compression*

Figure 6 shows, for the hydrostatic compression tests, the volume change against the logarithm of elapsed time. With increasing effective consolidation pressure, the inclination of those curves increased and the volume change had not ceased after 24 hours. On the other hand, Figure 7 shows the same relationships, this time during unloading, and it is apparent that there is an increase in the inclination of the curve with decreasing effective consolidation pressure.

After testing, we measured the particle-size distributions (PSD) which are shown in Figure 4. It is seen that the PSD before and after hydrostatic compression tests are not much different, indicating that excessive particle crushing did not occur within the applied effective consolidation pressure of 1600 kPa.

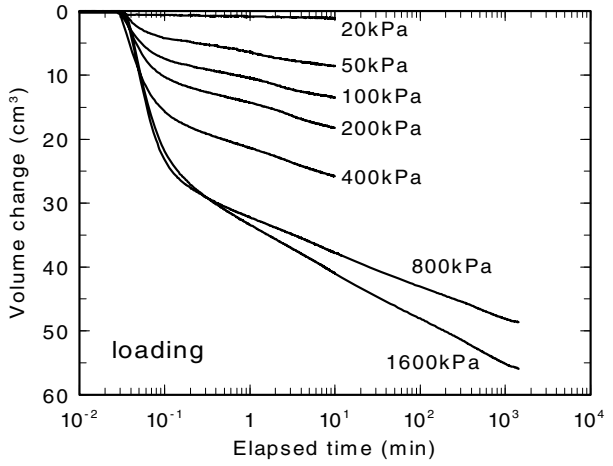

Figure 6. Volume change against elapsed time during hydrostatic compression.

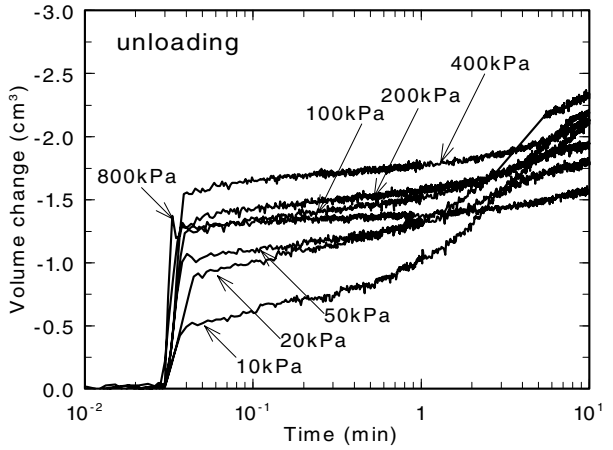

Figure 7. Volume change against elapsed time during unloading under hydrostatic compression.

3.2 *K_o compression and stress relaxation*

Figure 8 shows the time history of axial stress normalised with respect to the maximum axial effective stress reached in each test. The curves during the constant deformation stress relaxation for the loose samples show slightly more decrease in vertical effective stress than those for the dense samples. These differences between the stress relaxation for loose and dense samples increased with increasing displacement rate during the initial constant deformation rate testing for the specimens.

Secondly, particle crushing of pumice sand was measured. It is clear from Figure 4 that particle crushing occurred during K_o testing. Even though the effective vertical stresses are not the same in hydrostatic compression and K_o testing (the maximum axial stress in the hydrostatic compression tests was 1600 kPa and that for K_o testing of the loose sample at lowest displacement rate was 3000 kPa), a more likely explanation is that shear stress induces more particle crushing than hydrostatic stress. Based on the work of Hardin (1985), the total breakage, B_t, was calculated as the area enclosed by PSD curves before and after testing and the vertical line corresponding to 0.063 mm (the line defined by Hardin was 0.074mm). As shown in Figure 9, B_t increases with increase in the maximum shear stress.

We should like to offer a tentative explanation as to why constant displacement stress relaxation is influenced both by the prior displacement rate and density of the sample. It is believed that if the maximum displacement and the displacement rate are large, the stress at each contact point is large because the displacement rate is so fast that particle movement is inhibited. Therefore, the stress distribution inside the specimen becomes more non-uniform with increasing displacement rate. Then, during stress relaxation, the stresses at contact points can decrease and the particles tend to adjust to more stable positions. This means that non-uniformity of stress distribution inside the specimen may be reduced during stress relaxation.

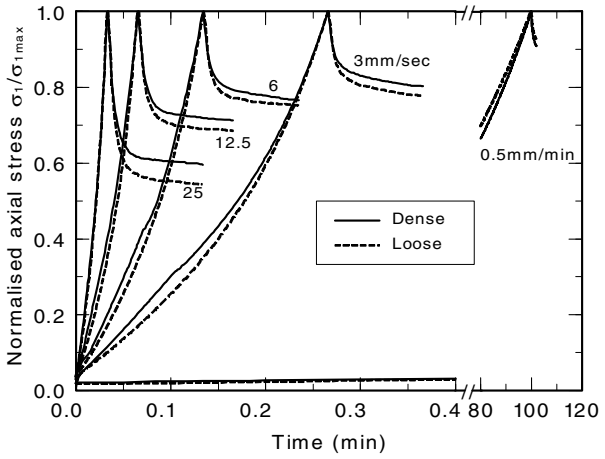

Figure 8. Relationship between normalised axial stress and time.

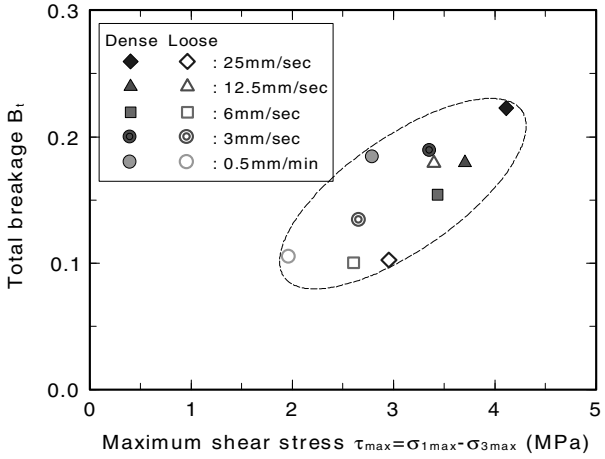

Figure 9. Relationship between total breakage and maximum axial stress.

4 CONCLUDING REMARKS

In this study, hydrostatic compression and K_o compression and post-peak stress relaxation testing were performed on loose and dense pumice sand.

It was found that although there was substantial volume change of the pumice sand during hydrostatic compression negligible particle crushing occurred in these tests. On the other hand substantial particle crushing was induced during the K_o compression.

The effects of density, displacement rate and particle crushing on compression and stress relaxation were investigated. From the K_o test results, it was observed that the amount of post-peak stress relaxation increased with increasing displacement rate and the differences between the stress relaxation in loose and dense pumice sands increased with increasing displacement rate. This means that it might be possible to evaluate the density of pumice sand through the magnitude of stress relaxation during CPT sounding, e.g., since CPT testing is usually carried out at a displacement rate of 20 mm/sec, CPT penetration can be stopped for a while and the decrease in q_c value recorded for several minutes to evaluate the magnitude of stress relaxation.

ACKNOWLEDGMENT

The first named author is very grateful to the New Zealand Earthquake Commission for support.

REFERENCES

Davis, E. H. & Poulos, H. G. 1964. Triaxial testing and three-dimensional settlement analysis, *Proc., Fourth Australian-New Zealand Conference on Geomechanics*, 233-243.

Hardin, B. O. 1985. Crushing of soil particles, *Journal of Geotechnical Engineering*, Vol. 111, No. 10, 1177-1192.

Kikkawa, N., Pender, M. J. and Orense, R. P. 2008. Visualisation of soil particles in Auckland residual soil using X-ray CT scanning, *Proc. of the 6th Asian Young Geotechnical Engineers Conference*, Bangalore, India, 6pp.

New Zealand Standard. 1988. NZS 4402 : 1988 : Section 4.2 Determination of the minimum and maximum dry densities and relative density of a cohesionless soil.

Pender, M. J. 2006. Stress relaxation and particle crushing effects during K_o compression of pumice sand, *Proc., International Symposium on Geomechanics and Geotechnics of Particulate Media,* Yamaguchi, Japan, 91-96.

Wesley, L. D., Meyer, V. M., Pronjoto, S., Pender, M. J., Larkin, T. J. & Duske, G. C. 1999. Engineering properties of pumice sand. *Proc. 8th Australia-NZ Conference on Geomechanics*, Vol. 2, 901-908.

Wesley, L. D. 2001. Determination of specific gravity and void ratio of pumice materials, *Geotechnical Testing Journal*, 24 (4), 418-422.